OPEN ACCESS

University of BRISTOL

Foo, S. E., & Beach, M. A. (2002). Uplink based downlink beamforming in UTRA FDD. (pp. 12 p).

Link to publication record in Explore Bristol Research

PDF-document

## University of Bristol - Explore Bristol Research

### General rights

SOURCE:        Centre for Communications Research,
               University of Bristol, UK.

**Uplink based Downlink Beamforming in UTRA FDD**

S. E. Foo and M. A. Beach
Queen's Building,
University Walk, Clifton,
Bristol.
BS8 1TR. UK.
Phone: +44 117 928 8617
Fax:     +44 117 954 5206
Email: s.e.foo@bris.ac.uk

# Uplink based Downlink Beamforming in UTRA FDD

S. E. Foo and M. A. Beach

Centre for Communications Research,
University of Bristol, UK.
*Email: s.e.foo@bris.ac.uk.*

## Abstract

Smart Antennas offer a unique solution for increased spectrum efficiency in future mobile radio communication systems. In FDD applications, uplink weights are not applicable on the downlink due to the duplex separation bandwidth. In the absence of downlink channel information, the direction of arrival of prominent signals can be estimated to provide a beamforming direction for transmission. This paper presents the results of a simulation to evaluate the performance of such beamforming approaches based on numerous DOA estimation techniques in the presence of grating lobes, using actual measured channel responses for UTRA FDD.

## 1 Introduction

Smart antennas promise to provide increased spectral efficiency to meet the ever increasing demands of future generation mobile cellular systems. Range extension and capacity enhancement is achieved via spatial processing offered by the use of multi sensor arrays together with a beamformer [1].

Whilst it is possible to employ Smart Antennas at both the basestation and mobile equipment, the additional hardware complexity and consequent power requirements of this configuration is less feasible at the mobile terminal due to physical size and battery life constraints. Therefore, the deployment of array architectures are more common place at the basestation.

In the uplink reception at the basestation, spatial knowledge of the channel is available thus facilitating the exploitation of the spatial component of the incoming signals. In the case of downlink transmission, the channel knowledge can be obtained from the uplink reception in Time Division Duplex (TDD) systems, provided the duplex time is within the coherence time of the channel such that the channel statistics remain constant for the downlink transmission. However, in Frequency Division Duplex (FDD) system, such channel reciprocity is not valid if the duplex spacing is greater than the coherence bandwidth of the channel. In Universal Terrestrial Radio Access (UTRA) FDD deployments where a nominal spacing of 190MHz is employed between the downand uplink, the beamformer is unable to reuse the weights from reception for transmission beamforming.

In order to investigate the channel de-correlation between the downand uplink, numerous channel sounding campaigns have been performed in the UTRA FDD bands [2, 3].

This paper presents a statistical analysis of the beamformer gain from a simulation of an eight element Uniform Linear Array narrowband beamformer (weights remain constant throughout the duration of the impulse response) in the presence of grating lobes using measured channel responses from [3]. Temporal processing of the signals is typically done in Code Division Multiple Access (CDMA) systems by the Rake receiver, and when used with a narrowband Smart Antenna, offers an attractive though sub-optimal alternative to a space time processor in terms of reduced system complexity and cost.
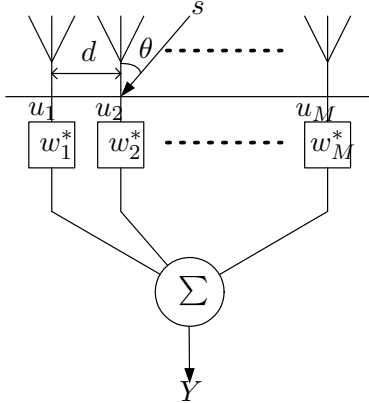
Figure 1: Beamformer

## 2   Signal Model

Figure 1 shows an $M$-element array with inter-element spacing $d$ and weight $w_m$ corresponding to element $m$ where $(\cdot)^*$ denotes complex conjugation. Here, we consider the case of a single signal, $s$, impinging on the array at angle $\theta$ from boresight (neglecting elevation) corresponding to the most powerful component, which is from the desired user. It is assumed that the bandwidth of the signal is small compared to the carrier frequency such that the phase difference seen by different array elements are strictly due to the geometry of the array and $\theta$.

The signals from each element for a signal impinging from angle $\theta$ is given by (1),

$$
\begin{aligned}
\mathbf{U}(\theta) &= As \begin{bmatrix} 1 \\ e^{-j\frac{2\pi}{\lambda}dsin\theta \cdot (1)} \\ \vdots \\ e^{-j\frac{2\pi}{\lambda}dsin\theta \cdot (M-1)} \end{bmatrix} \\
&= As\mathbf{a}(\theta)
\end{aligned}
\tag{1}
$$

where $A$ is the complex coefficient of the channel at that instant (which is constant for all the elements), $\lambda$ is the wavelength and $\mathbf{a}(\theta) = [\ 1 \quad e^{-jk} \quad \cdots \quad e^{-jk(M-1)}\ ]^T$ is the steering vector corresponding to azimuth $\theta$ and $k = \frac{2\pi}{\lambda}dsin\theta$.

The output of the beamformer is given by (2). Here, only phase weights are used, thus the amplitude of the weights are unity.

$$
\begin{aligned}
y &= \mathbf{w}^T\mathbf{U} \\
&= As\mathbf{w}^T\mathbf{a}
\end{aligned}
\tag{2}
$$

where $(\cdot)^T$ denotes transposition. The weights are given by $\mathbf{w} = [\ w_1^* \quad w_2^* \quad \cdots \quad w_M^*\ ]^T$. It can be seen that the output of the beamformer, $y$ is maximum when $\mathbf{w} = \mathbf{a}$. Therefore, to form a beam towards a desired azimuth angle, the complex conjugate of the steering vector for that array is the appropriate weight to use. This weight can either be calculated assuming an ideal array response, or measured by performing an array calibration as performed here so that mutual coupling effects are taken into account.
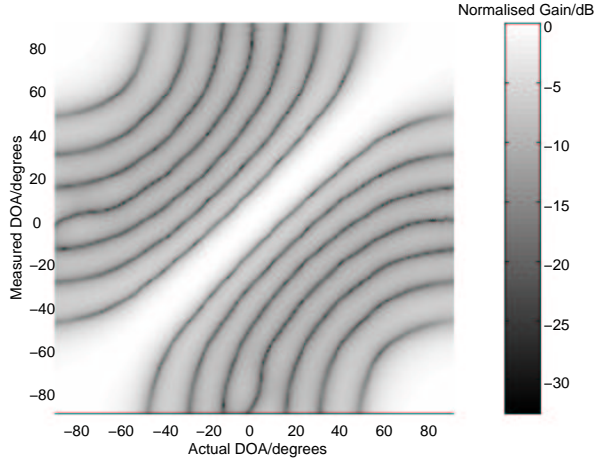
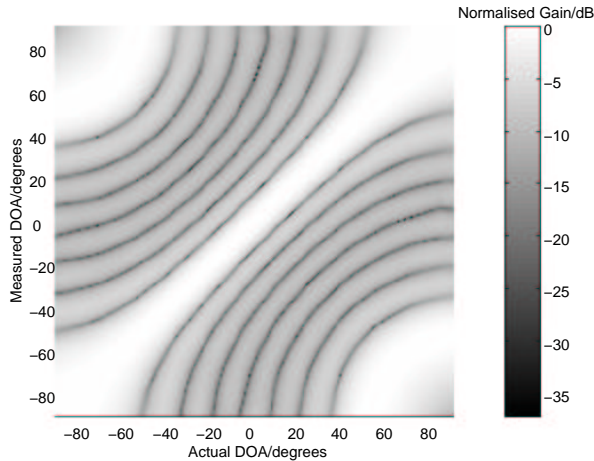Figure 2: Beamforming Errors at 1.9GHz due to Grating Lobes



Figure 3: Beamforming Errors at 2.1GHz due to Grating Lobes

# 3  Array Calibration and DOA Estimation

The array used for the simulations is a custom build Universal Mobile Telecommunications System (UMTS) eight element Uniform Linear Array (ULA) by Allgon Systems AB (Figure 4). This had an inter-element spacing of $0.512\lambda$ and $0.56\lambda$ for the upand downlink frequencies respectively (1.92GHz, 2.12GHz). This gives rise to grating lobes that appear when the beamforming angle exceeds approximately $50°$ as given by (3) [4], where $\theta_{bf}$ is the beamforming azimuth and $\theta_g$ is the grating lobe azimuth. On the uplink, ambiguities in Direction of Arrival (DOA) estimation occur at around $70°$ azimuth.

$$\frac{d}{\lambda}(sin\theta_g - sin\theta_{bf}) = \pm n \tag{3}$$

The weights used for the Fourier method of DOA estimation on the uplink and for beamforming on the downlink were from array manifolds measured separately in an anechoic chamber at both frequency bands. The array was rotated from $-90°$ to $+90°$ in the azimuth plane in $1°$ steps. The
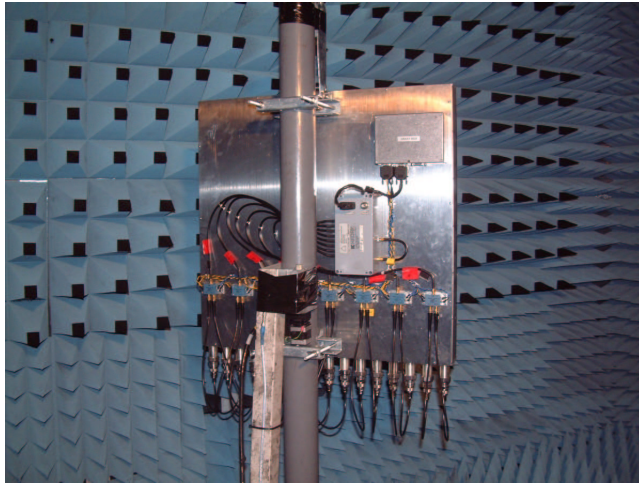
Figure 4: Receiving Array

elevation was maintained at $0°$.

Figures 2 and 3 show the plots of the of the actual DOA/targetted beamforming direction vs obtained Power-Azimuth Spectrum (PAS) for the upand downlinks respectively. The plots were obtained by evaluating $M^{\dagger} * M$ where $M$ is the 8 by 181 measured array manifold and $(\cdot)^{\dagger}$ denotes complex conjugated transpose. The light diagonal that runs across the figures corresponds to the output PAS reflecting the correct DOA but the light corners at the top left and bottom right show the errors/ambiguity due to grating lobes. Looking across the horizontal, the dark stripes corresponds to the seven nulls obtained when beamforming with an eight element array.

# 4   Channel Measurements

The channel data used here was measured in the city of Bristol. The environment consists of a mixture of urban city centre and an urban residential area (see Figure 5). The terrain is fairly built up and hilly, with streets between one to three lanes wide. The basestation was located on the roof of a building with a height of approximately 30m from ground level. The site of the building was elevated and the receiving array had a good aerial view of the area.

Figure 6 shows the map of the location. Five drive tests were performed with the array pointing at a bearing of $330°$ for Routes One and Two, and $240°$ for Routes Three, Four and Five. They span a total measurement time of approximately 30 minutes and cover a distance of approximately 10km. The routes comprise a mixture of arc and radial paths from the basestation and were performed during the day time to obtain a most representative response of an urban environment. The dynamic nature of the measurements thus simulate the effect of a moving mobile user in a city environment.

The channel sounder used was the state of the art Medav RUSK BRI [5], which was further customised to perform dual band channel sounding at the FDD bands.

Dedicated power amplifiers provided a total transmit power of +40dBm per frequency band via a 2dBi gain omni directional sleeve dipole antenna. The transmitting antenna was mounted on the roof of the trials vehicle to excite both channels simultaneously during the drive route measurements. A back to back calibration was performed prior to each deployment to ensure accurate time of flight and complex channel response by removing the response of the measuring equipment.

Figure 5: Typical Residential Environment

The receiving array then sampled the signals arriving at the basestation spatially, and systematically switched between elements and frequency bands. The Medav receiver was customised to sample at both frequency bands in a rapid sequential manner such that the channel statistics remain constant for each sampling of the frequency bands.

The resultant total data consists of 1087 instantaneous snap shots of the channel for each band, with a sampling interval of approximately 1.75s. The uplink channel sounding was performed at an RF frequency of 1910-1930 MHz and the downlink was performed at 2110-2130 MHz. For each band, each snap shot consists of eight sets of channel response vectors recorded back to back to provide stationary data for averaging to improve the signal to noise ratio. Every snap shot was recorded within a period of roughly $1.6ms$. Each set of channel response vectors in turn comprise of the complex frequency response as seen by each of the eight receiving elements and were recorded within a period of $102.4\mu s$. The resultant impulse response seen at each element spans $6.4\mu s$.

Figure 7 shows the PAS obtained from a five minute sample taken from the Route 1 drive test on the uplink. The parameters were estimated from the ESPRIT algorithm where a 25dB cutoff threshold from the most powerful component was applied. Figure 8 shows the counterpart at the downlink channel. It can be seen that there are estimation errors from approximately 80s to 130s on the downlink due to grating lobes as the magnitude of the incoming DOA was beyond $60°$. However, it is also seen that the dominant DOA's for each channel remains largely similar although the spread is different. It should be noted here that in an effort to clarify the plots, only the five most powerful estimates were included for each sample in time.

## 5 Simulation

One method to perform transmit beamforming at the basestation is to estimate the DOA on the uplink during reception and to use the dominant DOA for transmission [6].

This assumes that the DOA's of the signals are identical between the two channels [7], which is a valid assumption since the physical propagation mechanism for the channel varies insignificantly for such separations. Thus, provided the observations were performed within the period in which the
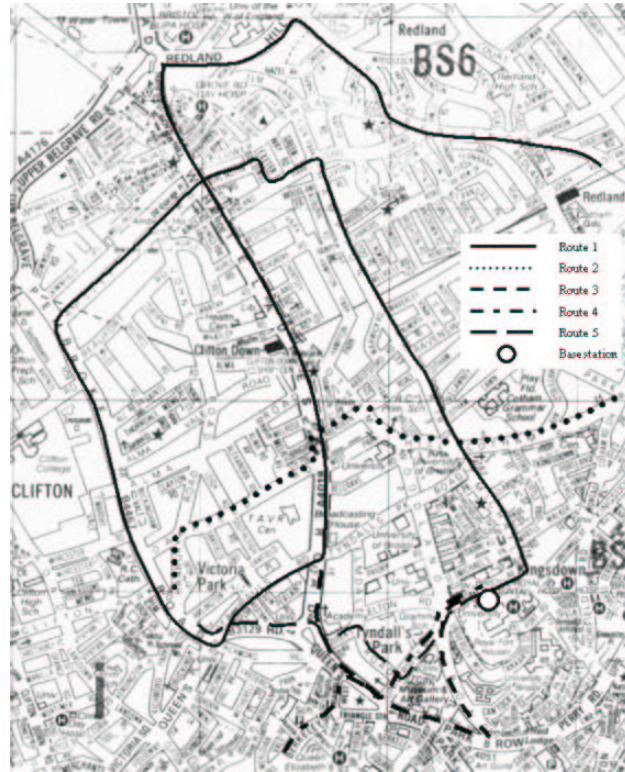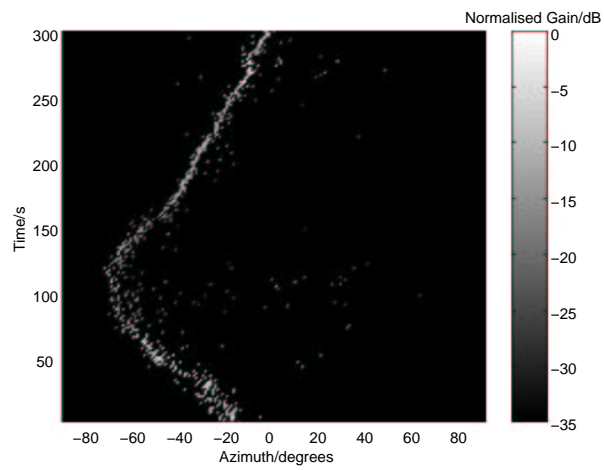
Figure 6: Measurement Routes



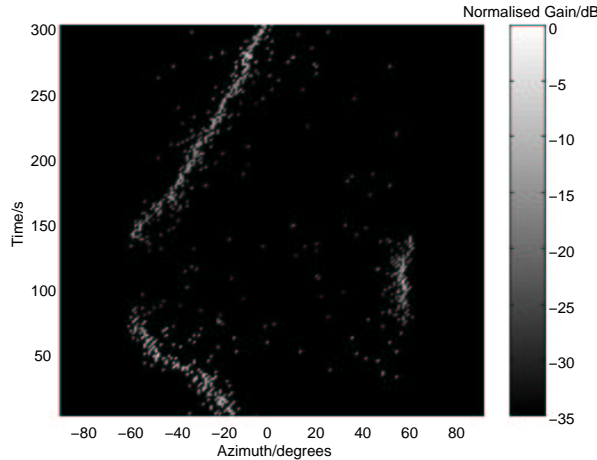Figure 7: Power Azimuth Spectrum for 1.92GHz Band

6

Figure 8: Power Azimuth Spectrum for 2.12GHz Band

channel is temporally stationary, the number of multipath componenets and their corresponding delay and azimuth parameters are constant for both channels.

However, the instantaneous fading (Rayleigh) as seen by both channels will be different due to the differences in wavelengths and finite resolution bandwidth. As such, both channels will fade independently.

For each snap shot, the DOA was estimated with several algorithms on the uplink. The classical Fourier method was implemented using the array manifold mentioned above but with three different settings. Fourier Wide Band (FWB) uses the full bandwidth of 20MHz and Fourier Medium Band (FMB) uses a bandwidth of 5MHz to average out frequency selective fading. Essentially, the PAS was evaluated for each frequency line and the magnitudes of these PAS were then averaged to obtain a more representative version which is independent of fast fading. Finally, Fourier Narrow Band (FNB) uses a single center frequency line (1.92GHz) in the computation of the PAS. The weight used for beamforming on the downlink was selected by searching for the peak in the resultant PAS of the uplink.

For the sake of comparison, super resolution parameter estimations were also employed to find the dominant DOA. Namely, the Space-Alternating Generalised Expectation-maximisation (SAGE) [8] and Estimation of Signal Parameters via Rotational Invariance Techniques (ESPRIT) [9] algorithms. Here, both algorithms were fed the full 20MHz of bandwidth.

## 6    Results

Table 1 shows the beamformer's gain using the five different techniques compared to the maximum possible gain obtainable. The optimum gain was evaluated by selecting the weight which yielded the highest output on the downlink. In reality, this is not possible since the response of the downlink channel is unknown at the basestation and thus can only be estimated from the uplink DOA.

It can be seen that on average, the Fourier method yields a more consistently closer result to that of the optimal solution compared to super resolution techniques. This is possibly due to the fact that even for cases where the uplink DOA estimation was degraded by grating lobes, in practice, the grating lobe problem is even more severe on the downlink (due to its higher frequency) and thus steering a beam towards the direction of the grating lobe actually produces a higher output

| Method | Max/dB | Min/dB | Mean/dB | Std. Dev./dB |
|---|---|---|---|---|
| FWB-Loss | 4.88 | 0.00 | 0.15 | 0.50 |
| FMB-Loss | 5.20 | 0.00 | 0.22 | 0.62 |
| FNB-Loss | 7.66 | 0.00 | 0.39 | 0.99 |
| SAGE-Loss | 9.67 | 0.00 | 0.57 | 1.20 |
| ESPRIT-Loss | 12.04 | 0.00 | 0.35 | 0.96 |

Table 1: Loss Statistics compared to Optimum Gain

| Method | Max/dB | Min/dB | Mean/dB | Std. Dev./dB |
|---|---|---|---|---|
| Opt-Gain | 9.28 | 2.94 | 8.29 | 0.68 |
| FWB-Gain | 9.27 | 2.33 | 8.14 | 0.86 |
| FMB-Gain | 9.27 | 1.92 | 8.07 | 0.94 |
| FNB-Gain | 9.27 | -0.66 | 7.90 | 1.30 |
| SAGE-Gain | 9.26 | -1.09 | 7.72 | 1.39 |
| ESPRIT-Gain | 9.19 | -3.20 | 7.94 | 1.18 |

Table 2: Gain Statistics for Simulation Results

than towards the true DOA. The super resolution methods probably chose a weight corresponding to the actual DOA and as such, suffers a slightly lower gain.

Table 2 shows the possible array gain obtainable from these techniques as well as the optimum array gain. As expected for an eight element array, the maximum gain obtainable is about 9dB. The improvement in performance between the wide band Fourier Method (20MHz-FWB) and the medium band Fourier Method (5MHz-FMB) is not as significant as the enhancement from the narrow band Fourier Method (single frequency line-FNB) to FMB. Similar performance improvements can be expected from an actual UTRA FDD implementation where the bandwidth is 5MHz with a chipping rate of 3.84Mcps [10]. Although the average gains for each case is largely comparable, it should be noted that the trend going down the minimum gain column highlights the possibilty of instantaneous losses. In some of the cases, the use of a beamformer actually gave a momentary loss over a single element antenna.

Figure 9 shows the discrepancies between the estimated DOA on the uplink and the optimum direction for beamforming on the downlink. Essentially, it shows the differences in estimated DOA on the uplink using the five techniques and the estimated DOA on the downlink using the Fourier Method using the full 20MHz bandwidth.

For up to 90% of the time, the differences are below $10°$. The second incline of the curve at approximately $130°$ is due to grating lobes. This is the scenario where on one link the correct DOA is estimated but on the other, the direction of the grating lobe has been detected as the DOA.

In Figure 10, it is shown how the five different means of obtaining weights for beamforming compare against each other by evaluating the difference in array gain for each case relative to the optimum case. For nearly 90% of the time here, the resultant gain was no more than 1dB below the optimum solution. This highlights the suitability of performing uplink-based downlink-beamforming, even in urban environments and when the links are spaced 200MHz apart.
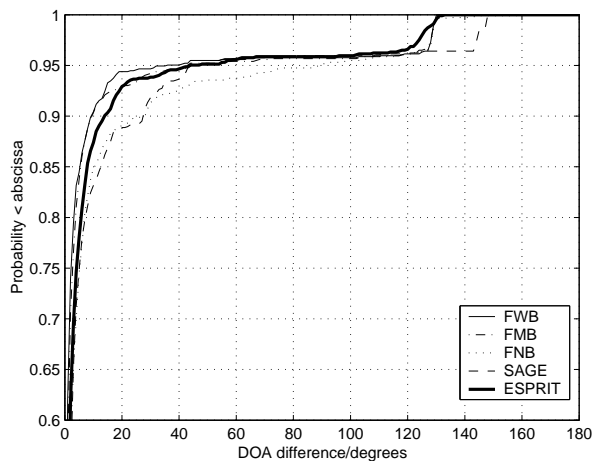
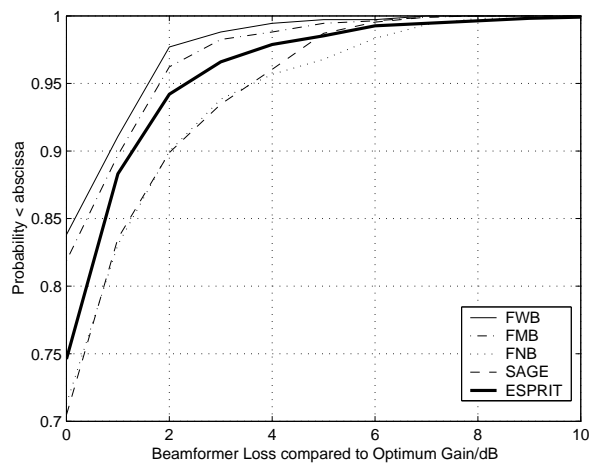Figure 9: CDF of differences in estimated DOA on uplink to optimum beamforming angle on downlink



Figure 10: CDF of beamforming loss compared to optimum beamforming gain

9

# 7 Conclusions

It is shown here that overall, the application of an eight element Smart Antenna in a typical urban environment representative of a UTRA FDD deployment in city centres can provide on average, around 8dB of gain over a single antenna scenario. This gain is seen on the downlink by utilising spatial information from the uplink, specifically the dominant DOA.

It is also shown that the DOA's between channels separated by 200MHz are virtually identical, despite the channels fading independently. As such, it is desirable to perform uplink-based downlink-beamforming in such FDD systems.

The performance edge over conventional Fourier Method for DOA estimation of super resolution techniques does not justify their additional computational complexity. In fact, with the presence of grating lobes, the Fourier Method offered better performance from the point of view of maximising the array output (lower transmit power requirement for given SNR level).

Finally, the robustness of such systems is proven from the results obtained where performance degradation over the optimal solution was no more than 1dB for 90% of the time.

# 8 Acknowledgements

# References

[1] J. C. Liberti and T. S. Rappaport, *Smart Antennas for Wireless Communications: IS-95 and Third Generation CDMA Applications.* Prentice Hall, 1999.

[2] K. Hugl, *Spatial Channel Characteristics for Adaptive Antenna Downlink Transmission.* Ph.D. Thesis, Vienna University of Technology, 2002.

[3] S. E. Foo, M. A. Beach, P. Karlsson, P. Eneroth, B. Lindmark and J. Johansson, *Spatioa-Temporal Investigation of UTRA FDD Channels.* Proc. IEE 3G Mobile Communication Technologies 2002, pp. 175–179.

[4] M. I. Skolnik, *Introduction to radar systems*, 2nd edition, McGraw Hill 1980, Chapter 8 pp. 283.

[5] R. S. Thom'a, D. Hampicke, A. Richter, G. Sommerkorn, A. Scneider, U. Trautwein and W. Wirnitzer *Identification of Time-Variant Directional Mobile Radio Channels* IEEE Trans. Inst. and Meas., Vol. 49, pp.357–364.

[6] M. Bengtsson and B. Ottersten, *Optimal and Suboptimal Transmit Beamforming* Handbook of Antennas in Wireless Communications, edited by L.C. Godara, CRC Press, 2001.

[7] J. H. Winters, *Smart Antennas for Wireless Systems* IEEE Personal Communications, February 1998.

[8] B. H. Fleury, D. Dahlhaus, R. Heddergott and M. Tschudin, *Wideband Angle of Arrival Estimation Using the SAGE Algorithm* Proc. IEEE 4th Int. Symp. on Spread Spectrum Techniques and Applications (ISSSTA '96) Mainz, Germany, 1996, pp. 22–25.

[9] R. Roy and T. Kailath, *ESPRIT Estimation of Signal Parameters via Rotational Invariance Techniques*, IEEE Trans. ASSP, Vol. 37 No. 7, July 89, pp. 984–995.

[10] 3rd Generation Partnership Project(3GPP), *Technical Specification Group Radio Access Networks; UE Radio Transmission and Reception (FDD)* 3GPP TS 25.101 v5.2.0, www.3gpp.org, 2002.